Innovative Food Science and Emerging Technologies 16 (2012) 398–408

Contents lists available at SciVerse ScienceDirect

Innovative Food Science and Emerging Technologies

journal homepage: www.elsevier.com/locate/ifset

Analysis of membrane fouling during cross-flow microfiltration of wine

Youssef El Rayess [a,b,*], Claire Albasi [a,b], Patrice Bacchin [c,d], Patricia Taillandier [a,b], Martine Mietton-Peuchot [e,f], Audrey Devatine [e,f]

[a] Université de Toulouse, INPT, UPS, Laboratoire de Génie Chimique, 4 Allée Emile Monso, F-31432 Toulouse, France
[b] CNRS, Laboratoire de Génie Chimique, F-31432 Toulouse, France
[c] Université de Toulouse, INPT, UPS, Laboratoire de Génie Chimique, 118 Route de Narbonne, F-31062 Toulouse, France
[d] CNRS, Laboratoire de Génie Chimique, F-31062 Toulouse cedex 09, France
[e] Université de Bordeaux, ISVV, EA 4577, Unité de recherche OENOLOGIE, 33882 Villenave d'Ornon, France
[f] INRA, ISVV, USC 1219 OENOLOGIE, 33882 Villenave d'Ornon, France

ARTICLE INFO

Article history:
Received 3 April 2012
Accepted 8 September 2012

Editor Proof Receive Date 5 October 2012

Keywords:
Cross-flow microfiltration
Fouling
Wine
Tannins
Pectins
Mannoproteins

ABSTRACT

The aim of this study was to investigate the individual impact on wine molecules as tannins, pectins and mannoproteins on multichannel ceramic membrane fouling during wine cross-flow microfiltration. The characterization of fouling mechanisms involved in the previous filtrations was realized by using the classical fouling models and the analysis of the total resistance curves. It was shown that the obtained initial fluxes are dependant of the nature of the studied molecules and their concentration. According to their increasing effect on permeate flux decline, the studied wine components could be ranked as: mannoproteins < tannins < pectins. During the filtration of wine added with tannins, it was found that the filtrations were governed by the cake layer formation mechanism. The presence of pectins caused the formation of gel-type layer which is found to be compressible under high pressures. For wines added with mannoprotein filtrations, it was shown that there is a threshold concentration above which a plateau value of permeate flux is obtained.

Industrial relevance: The cross-flow microfiltration applied to wine filtration has become a legitimate alternative to conventional filtration processes. However, membrane fouling which affects the operating costs and the plant maintenance, limits the widespread application of this technique. To avoid or reduce membrane fouling, it is extremely important to identify the fouling elements and the mechanisms that govern the process. A better understanding of the mechanisms whereby fouling is formed during wine microfiltration may lead to be in position to control fouling or reduce it, to improve cleaning procedures and to adapt the process to the product to be filtered.

The results presented in this paper concern the investigation and the understanding of fouling mechanisms by wine colloids (tannins, pectins and mannoproteins). We found that wine colloids had a strong impact on membrane fouling. Independently of their concentrations found in wine, they can be ranked according to their increasing effect on permeate flux as: mannoproteins < tannins < pectins. Such result provides important information and a better vision on the methods which can be used to limit membrane fouling for example the use of pectinolytic enzymes before filtration in order to hydrolyze pectin chains or precipitation of unstable tannins by finning the wine with bentonite. By elucidating fouling mechanisms such as cake layer and gel type layer, we can adapt the hydrodynamic process to control membrane fouling.

© 2012 Elsevier Ltd. All rights reserved.

1. Introduction

Clarifying wines using membrane filtration has begun to set up in oenology sector since the mid-1980s (Poirier, Bennasar, Tarodo de la Fuente, Gillot, and Garcera, 1984). Compared to the conventional clarification processes such as centrifugation, filtration on sheets, diatomaceous earth filtration, etc., cross-flow microfiltration can bring the following benefits such as the combination of clarification, microbiological stabilization and sterile filtration in one single continuous highly automated operation; and the elimination of the use of diatomaceous earth, thereby, reducing production costs and the problem of waste disposal leading to an improvement in work safety and production (El Rayess, Albasi, Bacchin, Taillandier, Raynal, et al., 2011).

Unfortunately, as in most other applications, the main problem in practical application of cross-flow microfiltration in wine industry is membrane fouling. It manifests by the reduction of permeate flux with time, caused by the wine components. This has caused difficulties in obtaining a competitive and economical productivity.

* Corresponding author at: Université de Toulouse, INPT, UPS, Laboratoire de Génie Chimique, 4 Allée Emile Monso, F-31432 Toulouse, France. Tel.: +33 534323900.
E-mail address: youssef.elrayess@ensiacet.fr (Y. El Rayess).

1466-8564/$ – see front matter © 2012 Elsevier Ltd. All rights reserved.
http://dx.doi.org/10.1016/j.ifset.2012.09.002

When filtering a biological fluid as wine and considering its complexity, membrane fouling can be attributed to three different mechanisms: i) concentration polarization and subsequent cake layer formation, ii) adsorption of solutes onto the membrane surface and pore walls, and iii) blockage of pores (Vernhet and Moutounet, 2002; El Rayess, Albasi, Bacchin, Taillandier, Mietton-Peuchot, et al., 2011a). Membrane fouling could also be divided according to its location relative to the membrane structure:

- *Internal fouling* is caused by the adsorption and deposition of small particles and macromolecules within the internal structure of the pores;
- *External fouling* is caused by the deposition of large macromolecules and particles on the top of membrane surface.

Research works concerning wine cross-flow microfiltration highlighted that wine macromolecules such as polyphenols, polysaccharides and proteins as well as wine particles as yeast, bacteria and cell debris are responsible of membrane fouling (Belleville, Brillouet, Tarodo de la Fuente, and Moutounet, 1992; Boissier, Lutin, Moutounet, and Vernhet, 2008; Salazar, de Bruijn, Seminario, Guell, and Lopez, 2007; Vernhet and Moutounet, 2002). Many researchers have demonstrated the negative effect of wine polysaccharides and polyphenols on the permeation flux especially by adsorption of these molecules on membrane materials (Belleville et al., 1992; Ulbricht, Ansorge, Danielzik, Konig, and Schuster, 2009; Vernhet and Moutounet, 2002). A recent study (Ulbricht et al., 2009) had provided evidence that different membrane materials exhibit various levels of adsorption of typical foulants in wine such as polysaccharides and polyphenols. Adsorption of these components is less on hydrophobic membrane than on hydrophilic membrane.

There have been numerous attempts to reduce membrane fouling by mechanical (back-flushing, back-pulsing and cross-flushing) and chemical cleaning. These steps are time consuming and add up mechanical and chemical stresses to the filtration devices resulting in a loss of capacity and efficiency of the equipment. Also, a main difficulty of wine cross-flow microfiltration is the non-reproducibility of pilot performances. The complexity of wine composition plays a major role and depends on the variability of the grapes and technological operations during the wine elaboration. The molecules/molecules and molecules/membrane interactions make the situation more complicated. To avoid or reduce membrane fouling, it is extremely important to identify the fouling elements and the mechanisms that govern the process. A better understanding of the mechanisms whereby fouling is formed during wine microfiltration may lead to be in position to control fouling or reduce it, to improve cleaning procedures and to adapt the process to the product to be filtered.

Nowadays, substances like polysaccharides, polyphenols and large particles are identified to be involved in the fouling process. However, studies to evaluate the contribution of each class of components present in the wine and the respective involved mechanisms in membrane fouling are still lacking. So, the aim of the present work was to investigate the relative impact of polyphenols (especially tannins) and polysaccharides (pectins and mannoproteins) on multichannel ceramic membrane fouling during a red wine cross-flow microfiltration and to identify the fouling mechanisms.

2. Theory

In this section, the clogging phenomena (adsorption, particle capture, deposit formation and biofilms) leading to the deposition of fouling material in/on the membranes are distinguished from the mechanisms limiting the transfer of material which they induce. The filtrations of complex solutions are characterized by the coexistence of different mechanisms whose relative contributions depend on the nature of the filter media, operating conditions and fluid characteristics. However, modeling the fouling phenomena allows the representation of fairly simple mechanisms to assist in the thinking of further practices. In fact, modeling is quite accurate to what is observed with microscopy techniques. The classical filtration models in microfiltration were originally developed by Hermans and Bredee (1936) and reviewed by Hermia (1982). Their use has the advantage of a non-ambiguous interpretation of often complicated fouling phenomena. These fouling phenomena limit the filtration of a complex solution like wine which contains molecular and colloidal fractions with large particle size distribution.

According to these models, four mechanisms are identified to reduce flow rate through the membrane (Fig. 1) (Bowen, Calvo & Hernandez, 1995; Hermia, 1982):

(a) Sealing the pore of the membrane (*complete blocking, n = 2*): according to this model, each particle, bigger than the pore diameter, is retained at the surface of the membrane and completely blocks the entrance of the pores. Moreover, the particles never settle on other particles which have been previously blocked by a pore.
(b) Partial blocking of pores (*intermediate blocking, n = 1*): this model considers that the inner pore walls are covered gradually and uniformly by molecules smaller than the pore size. This decreases the pore volume proportionally to the filtered volume. Therefore, the cross-section of the pores decreases over time.
(c) Internal pore blocking (*standard blocking, n = 3/2*): as well as the complete blocking model, this model assumes that the molecules block the entrance of the pores. But, it considers also that molecules can settle on the others previously retained by the membrane. This means that not all molecules approaching the surface of the membrane block a pore entrance.
(d) Formation of a deposit on the membrane surface (*cake formation, n = 0*): according to this model, a deposit or cake is formed on the membrane surface by the retained molecules which are considered bigger than the pore diameter. Cake thickness increases over time due to the stacking of molecules on the membrane surface.

These models have been developed for dead-end filtration with membranes having identical circular pores (identical pore diameter and length). The parameters considered by these models have a physical meaning and contribute to the comprehension of the mechanisms of membrane fouling. The four models are based on the laws only valid for constant pressure filtration and can be described by a common mathematical Eq. (1):

$$J = \frac{1}{S}\frac{dV}{dt}. \quad (1)$$

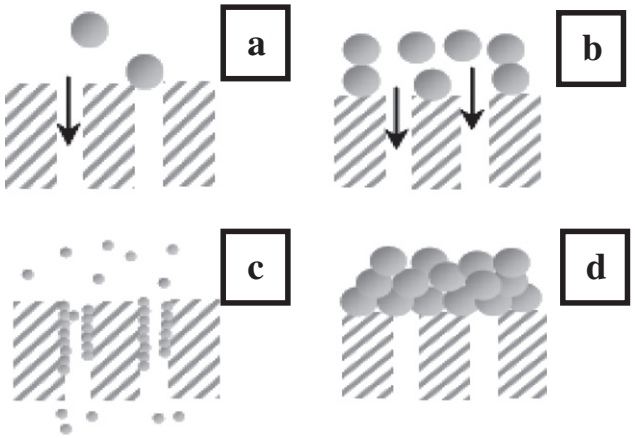

Fig. 1. Illustration of the fouling mechanisms considered by the blocking laws.

The representation of this equation in logarithmic scale gives directly the value of the obtained slope (n). The exponent n (blocking index) characterizes the filtration mechanism while k (resistance coefficient) allows the evaluation of the characteristic parameters of the retained model.

All these models and their characteristic and linearized equations are summarized in Table 1.

In the literature, experimental data for the flux decline have been often analyzed using the linearized forms. In most cases, the model which best fits with the experimental data is claimed to depict the fouling phenomena. However, filtration of the complex media is known to be the place of the coexistence of different fouling mechanisms. For that, the use of the common Eq. (1) offers the possibility to represent the four models of blocking in a single log–log plot where the log(dt/dV) represents the hydraulic resistance and $\log(d^2t/dV^2)$ the variation of the resistance with the filtered volume (Grenier, Meireles, Aimar, and Carvin, 2008). This approach was used because several authors (Nandi, Das, Uppaluri, and Purkait, 2009) have shown that the behavior of microfiltration membranes with regard to fouling phenomena cannot be described by a single blocking model all along the filtration. This plotting will help us to determine the coexistence of mechanisms during the investigation of the impact of wine molecules.

3. Materials and methods

3.1. Red wine

The red wine used in the present study was elaborated in 2008 at the cooperative cellar of Rabastens (France) with Duras, Fer Servadou and Syrah grape varieties.

In the cellar, the filtration was performed in a cross-flow microfiltration pilot plant using organic membranes with a pore size of 0.2 μm. When received, the wine is analyzed and maintained at 4 °C until experiments, in order to reach tartrate stabilization and to prevent microorganisms' development. Before using the wine for filtration experiments, a preliminary filtration is performed using the experimental pilot and membrane described in Section 3.4 in order to eliminate the potential potassium tartrate crystals and precipitates. This final step allows obtaining the filtered wine (FW). The characteristics of the filtered wine are the following: 12% as alcohol content, 3.6 as pH, 0.6 g/l as sugars (glucose + fructose), 0.1 g/l as malic acid and 0.1 NTU as turbidity.

3.2. Chemicals

Tannins (Biotan®), used as a model of wine tannins, were purchased from Laffort (Bordeaux, France). These tannins are proanthocyanidic tannins extracted from grape skin with instantaneous dissolving (mean degree of polymerization $DP_m \approx 5.5$). Pectins from citrus fruit were used as a model for grape polysaccharides. They were purchased from Sigma-Aldrich (Lyon, France). Mannoproteins (Mannostab®) were purchased from Laffort (Bordeaux, France) and used as a model of yeast polysaccharides. The concentrations of added molecules are chosen according to those found in wine and identified in the literature (Flanzy, 1998; Ribéreau-Gayon, Glories, Maujean, and Dubourdieu, 2006).

Table 1
The blocking models and their schematic representation.

Model	Characteristic equation	Linearized form	k
Complete blocking (n = 2)	$\frac{d^2t}{dV^2} = k_c.\left(\frac{dt}{dV}\right)^2$	$\ln J = \ln J_0 - K_c t$	$K_c = K_A J_0$
Standard blocking (n = 3/2)	$\frac{d^2t}{dV^2} = K_i.\left(\frac{dt}{dV}\right)^{3/2}$	$\frac{1}{J^{1/2}} = \frac{1}{J_0^{1/2}} + K_s t$	$K_s = 2\frac{K_B}{A_0} A J_0^{1/2}$
Intermediate blocking (n = 1)	$\frac{d^2t}{dV^2} = K_s.\left(\frac{dt}{dV}\right)^1$	$\frac{1}{J} = \frac{1}{J_0} + K_i t$	$K_i = K_A$
Cake filtration (n = 0)	$\frac{d^2t}{dV^2} = K_g.\left(\frac{dt}{dV}\right)^0$	$\frac{1}{J^2} = \frac{1}{J_0^2} + K_g t$	$K_g = 2\frac{K_D R_g}{J_0 R_m}$

J_0: initial permeate flux (m/s), J: permeate flux (m/s), A_0: initial membrane surface (m^2), A: membrane surface blocked at time t (m^2), R_m: membrane hydraulic resistance (m^{-1}), R_g: hydraulic resistance due to the cake formation (m^{-1}), K_A: blocked surface of the membrane per unit of filtered volume that flows through the membrane (m^{-1}), K_B: cross section blocked surface per unit of total volume that flows through the membrane (m^{-1}), K_D: cake surface per unit of total volume which flows through the membrane (m^{-1}).

3.3. Wine analysis

For wine component quantification, spectrophotometric analyses were carried out on an Agilent 8453 UV/VIS spectrophotometer. Total polyphenols in wine were estimated by the total polyphenol index (TPI) using the absorption at 280 nm and under 1 cm optical path. Color intensity (IC) is the sum of optical densities at 420 nm, 520 nm and 620 nm under 1 mm optical path. Total polysaccharides were determined using the modified Usseglio-Tomasset method based on the precipitation of the polysaccharides with ethanol (Usseglio-Tomasset, 1976). Total anthocyanins were determined according to the Ribéreau-Gayon method using the sodium bisulphite (Ribéreau-Gayon et al., 2006). Total tannins were also determined according to the Ribéreau-Gayon method by transforming the proanthocyanidins into anthocyanidins (Ribéreau-Gayon et al., 2006). Tannins were also analyzed using the method of thioacidolysis as described by Preys, Souquet, Meudec, Morel-Salmi, and Cheynier (2004). The measurements were performed with a UHPLC (DIONEX, Ultimate 3000 RSLC) and the used column was a Kinetex® PFP (Phenomenex). pH, alcohol content, malic acid, glucose and fructose concentration were determined on the wine by FTIR spectroscopy (Fourier Transform Infra-Red spectroscopy). Mannoproteins were determined using the total polysaccharide method. Wine viscosity is determined with a controlled-stress rheometer (AR-2000 ex). Turbidity measurements (NTU) were performed with a Eutech TN-100 turbidimeter (Eutech Instruments, Singapore).

3.4. Experimental apparatus

The filtrations were performed with a wine filtration pilot system (Fig. 2a) designed especially for this study and built by "PERA" Company (Florensac, France). A detailed account of the experimental setup was presented elsewhere (El Rayess, Albasi, Bacchin, Taillandier, Mietton-Peuchot, et al., 2011a).

The microfiltration module contains a multi-channel (44) ceramic membrane (BK-Kompact, Novasep, France) shown in Fig. 2b with average pore diameter of 0.2 μm. The total active membrane surface was 0.118 m^2, with an external diameter of 25 mm. The membrane constituted of ZrO_2/TiO_2 layers lying on monolithic TiO_2–Al_2O_3 support layer.

After each experiment, a 6 step procedure of chemical cleaning is adopted to regenerate the membrane. This procedure was presented in another work (El Rayess, Albasi, Bacchin, Taillandier, Mietton-Peuchot, et al., 2011a). It should be mentioned that the same membrane was used throughout all the experiments presented in this paper. The initial permeability of the used membrane is 1050 l/h.m^2.bar (3×10^{-4} m/s.bar). The membrane permeability is checked with osmotic water after chemical cleaning and must be equal or above 900 l/h.m^2.bar (2.5×10^{-4} m/s.bar) (at 20–22 °C). If this permeability is not reached, cleaning using several chemicals is then performed to regenerate the membrane and to reach the desired reference permeability of the membrane.

3.5. Microfiltration experiment procedure

Cross-flow microfiltration experiments were realized in order to investigate the respective impact of tannins, pectins and mannoproteins

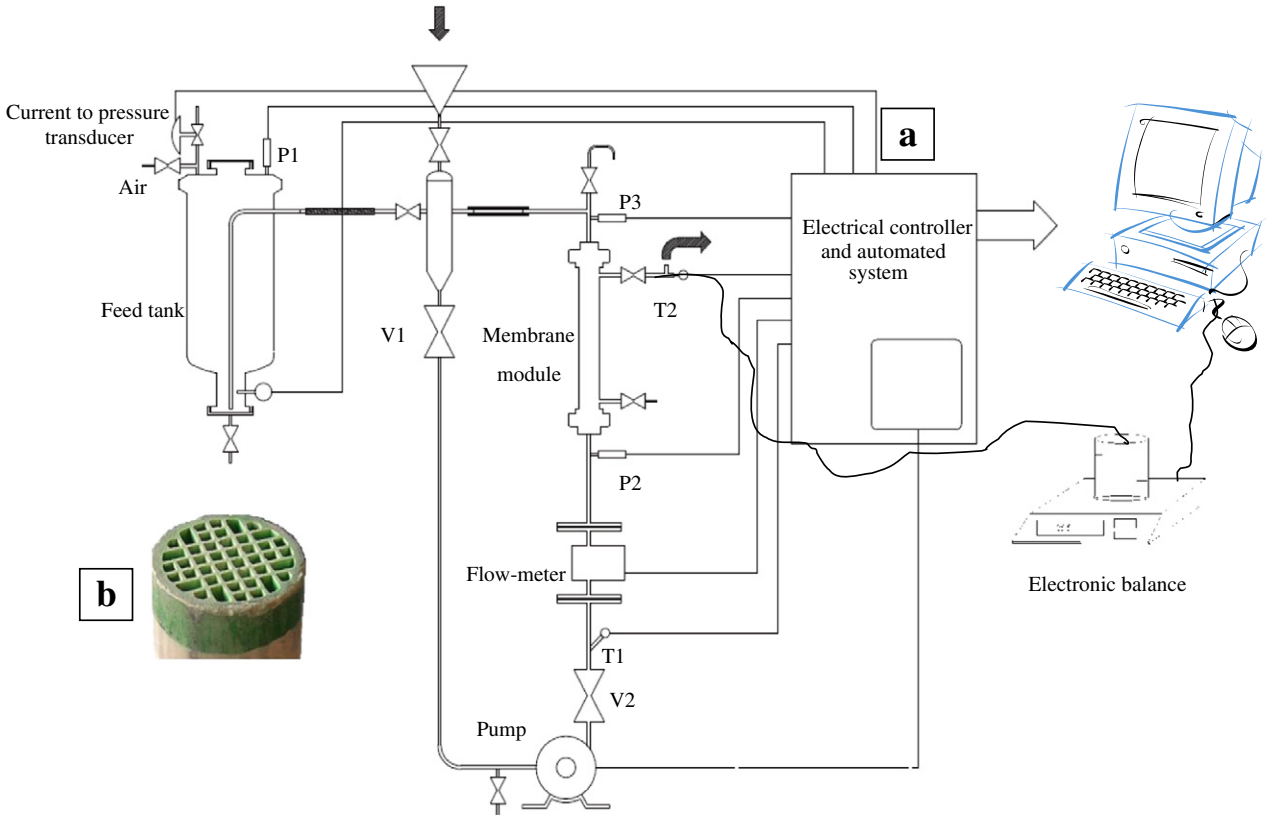

Fig. 2. a) Scheme of the experimental setup. b) Configuration of the multi-channel ceramic membrane (P = pressure sensor; T = temperature sensor).

on membrane fouling. The experiments were duplicated in order to check the repeatability of the obtained results. All experiments are repeatable (±5%) under the same conditions of concentration, transmembrane pressure, temperature and initial permeability of the membrane. To identify the fouling mechanisms, dead-end filtrations were carried out on the same membrane and in the same pilot as depicted in Fig. 2.

3.5.1. Cross-flow filtrations

The experiments consisted of constant TMP microfiltration runs. Each solution is filtered under two different pressures: 0.5 and 1×10^5 Pa. The impact of the different added molecules was studied for two chosen concentrations. Fig. 3 summarizes all conducted experiments and the imposed conditions.

All experiments were carried out with 10 l of the defined suspension. This volume was chosen in order to keep the volumetric reduction ratio (VRR) lower than 1.6. The solution to be filtered is placed in the feed tank and the circulation loop in order to expel the air from the loop. The flow velocity is fixed at 2 m/s which is conventionally used in wine filtration (without damaging the wine), corresponding to the Reynolds number equal to 2306 and 12.1 Pa as wall shear stress. According to René and Lalande (1991), the value of the Reynolds number corresponds to laminar flow regime.

Results of cross-flow filtrations will be presented as permeate flux function of filtered volume and total resistance function of filtered volume. Permeate flux (J) is calculated by Eq. (2).

$$J = \frac{1}{S}\frac{dV}{dt} \tag{2}$$

Total resistance (R) is expressed by the following expression:

$$R = \frac{\Delta P}{J.\mu}. \tag{3}$$

Where V is the filtered volume (m^3), t is the time (s), S is the membrane surface (m^2), ΔP is the transmembrane pressure (Pa) and μ is the wine viscosity (Pa.s).

3.5.2. Dead-end filtrations

To run in dead-end mode with this pilot, the pump was stopped and the valves V_1 and V_2 were closed. The circulation of the wine in the pilot is only provided by the pressurized air. Experiments were performed with 10 l of solution. The tested solutions and transmembrane pressures in dead-end mode are summarized in Fig. 4.

Results of dead-end filtrations will be firstly presented using the linearized forms detailed in Table 1. Then, they will be presented using the common mathematical equation.

4. Results and discussion

4.1. Effect of added tannins

4.1.1. Impact on cross-flow filtration performances

Fig. 5 shows the experimental data for the permeate flux as a function of filtered volume for filtered wines (FW) added with different concentrations of tannins (1.25 g/l and 2.5 g/l) filtered at 2 different transmembrane pressures (ΔP): 0.5 and 1×10^5 Pa. This figure shows also the permeate flux curves during the filtration of FW.

While filtering FW, the average permeate flux at 1 bar is about 1.8×10^{-4} m/s while it is about 0.83×10^{-4} m/s at 0.5×10^5 Pa. A little decrease in permeate flux is observed for both tested pressures. These results indicate that a weak fouling occurred even during the filtration of filtered wine. This fouling is mainly due to the adsorption of wine compounds on membrane material because the filtered wine doesn't contain particles or large macromolecules susceptible to form a deposit on membrane surface. This was checked by measuring the initial turbidity which was equal to 0.1 NTU. To highlight the

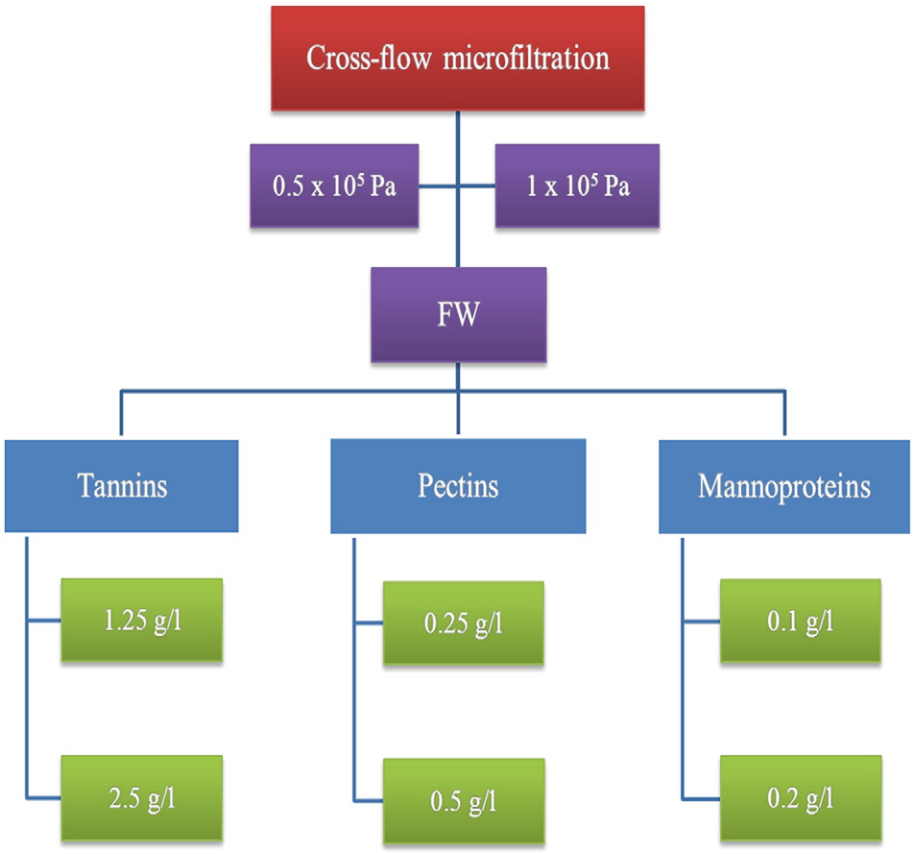

Fig. 3. A summary of cross-flow microfiltration experiments.

adsorption mechanism, the membrane was immersed in FW for 24 h and the water permeability was checked before and after immersion. A decrease about 10% of membrane permeability was measured. The adsorption mechanism was also proposed by Vernhet, Cartalade, and Moutounet (2003) to explain membrane fouling during filtration of the permeate of a red wine. For the following result analysis, this

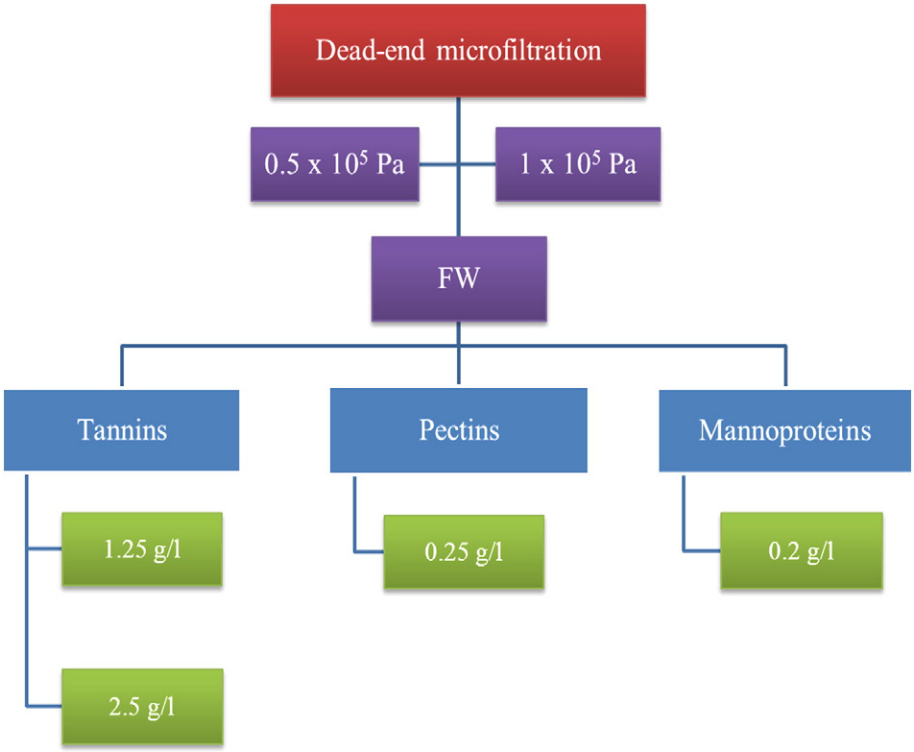

Fig. 4. Summary of dead-end microfiltration experiments.

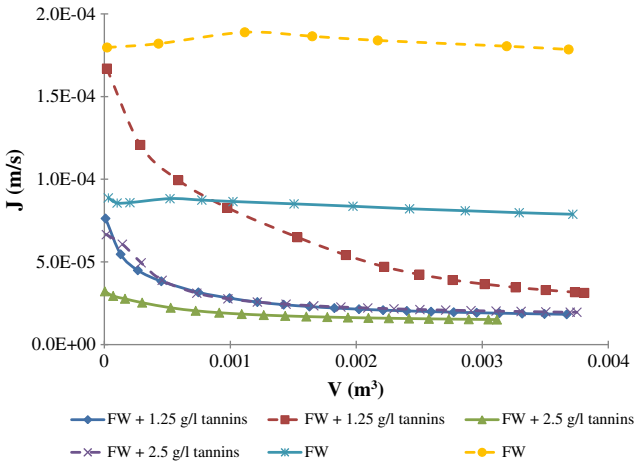

Fig. 5. Permeate flux profiles of FW wines loaded with different concentrations of tannins (—: 0.5×10^5 Pa; ---: 1×10^5 Pa).

10% variation due to adsorption will be considered in the error range of the flux measurements. Moreover this value has been obtained after 24 h of wine membrane contact while all the following experiments didn't last more than 80 min.

During the filtration of wines added with tannins, it can be seen that the lower permeate flux (1.9×10^{-5} m/s) was obtained with wines containing 2.5 g/l tannins. The impact of tannin concentration is noticeable while observing flux decreases. For the same pressure, wines containing 1.25 g/l tannins present higher fluxes than those containing 2.5 g/l tannins. The same behavior is reported by Czekaj, Lopez, and Guell (2000) who showed while filtering two white wines having the same initial turbidity that the different polyphenol concentrations of the 2 wines may explain the different performances observed during filtration.

It may also be observed that the permeate fluxes of wines loaded with tannins seem to stabilize around 2×10^{-5} m/s whatever the filtration conditions (pressure or concentration). This fact could be explained by the stabilization of the permeate flux by the cross-flow velocity independently of the transmembrane pressure.

Total resistance values calculated by Eq. (3) are plotted in Fig. 6 as total resistance versus filtrate volume. The total resistance, whatever the filtration conditions, increases during time; with a gradual decrease observed in slope during filtrations of FW + 2.5 g/l tannins at 0.5 and 1×10^5 Pa and FW + 1.25 g/l tannins at 0.5×10^5 Pa. According to Tracey and Davis (1994), an external fouling (pore blocking or cake formation) is represented by a curve with a decreasing slope and quasi-steady state of the resistance. Regarding more precisely the curves of FW + 2.5 g/l tannins, the external fouling is the dominant fouling mechanism. The filtration of wine containing 1.25 g/l tannins at 0.5×10^5 Pa presents the same mechanism. But the filtration of the same solution, FW + 1.25 g/l tannins, at 1×10^5 Pa suggests a shift from one mechanism to another and doesn't reach a quasi-steady state of the resistance.

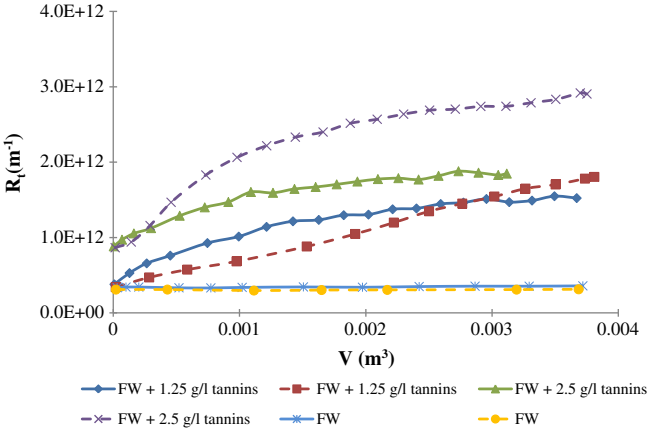

Fig. 6. Effect of tannin concentration and transmembrane pressure on total resistance (—: 0.5×10^5 Pa; ---: 1×10^5 Pa).

The contribution of tannin concentration and the pressure ΔP can be evaluated while plotting the total resistance versus filtered volume: at a given ΔP, an increase in tannin concentration led to a higher resistance while at the same concentration of tannins, the pressure impact is greater as the concentration is high. This observation may be explained by the increase of collision probabilities between tannin molecules forming bigger molecules, as the convective flux increased with pressure as far as the concentration increases. In fact, tannins have colloidal behaviors in wines and are unstable in wines which explain the changeable properties of tannins (Poncet-Legrand, Cartalade, Putaux, Cheynier, and Vernhet, 2003; Ribéreau-Gayon et al., 2006). During filtration, when increasing the ΔP, a gradient of the tannin volume fraction may appear from the suspension bulk to the surface of the membrane, which can cause tannin aggregation and eventually pore blocking and cake filtration in the neighbor of the membrane.

4.1.2. Fouling mechanisms

The identification of fouling mechanisms by wine tannins is realized by dead-end filtrations performed on the same multichannel ceramic membrane as the one used in the previous cross-flow filtrations. The decrease of permeate flux over time has been analyzed using the different filtration laws as discussed in Section 2. In the next paragraph, the linearized forms of blocking models are used. The results are investigated by plotting the common mathematical form (Eq. (1)) to check if the coexistence of mechanisms also exists during filtration of wine colloids.

4.1.2.1. Mechanism identification by linearized forms. To identify the most appropriate of blocking models to describe the decrease in permeate flux of FW + tannin filtration, the correlation coefficients (r^2) of different models are compared (Table 2). To confirm the model fitting, correlation coefficient (r^2) values should be greater than 0.99. As cake filtration model provided the highest values of r^2 (>0.99), this model was identified as the best fitted model to represent the flux decline mechanism for FW added with tannins independently from the transmembrane pressure and tannin concentration. Other models present r^2 values below 0.99. Therefore the resistance coefficient K_g has also been reported for this model. We can observe an increase in the resistance coefficient with the concentration, which is as expected. But, for a given concentration, the resistance coefficient decreases when the pressure increases, this implies that tannins form a non-compressible deposit on the surface of the membrane.

Table 2
Summary of parameters associated to various blocking models for FW added with tannins.

	Complete pore blocking	Intermediate pore blocking	Standard pore blocking	Cake filtration	
	r^2	r^2	r^2	r^2	K_g (s/m²)
FW + 1.25 g/l tannins (0.5×10^5 Pa)	0.9377	0.9769	0.9598	0.9959	1.85×10^6
FW + 1.25 g/l tannins (1×10^5 Pa)	0.9311	0.9805	0.9598	0.9981	1.00×10^6
FW + 2.5 g/l tannins (0.5×10^5 Pa)	0.9168	0.9795	0.9537	0.9999	5.10×10^6
FW + 2.5 g/l tannins (1×10^5 Pa)	0.9762	0.9731	0.9339	0.9999	3.95×10^6

4.1.2.2. Mechanism identification by d^2t/dV^2. As mentioned before, the obtained results with linearized forms will be checked by plotting the common mathematical equation for blocking models (Eq. (1)) (Fig. 7). The results show that only cake filtration (n = 0) occurs during filtrations of FW added with 1.25 g/l tannins regardless of the transmembrane pressure. The obtained results are consistent with those obtained with the cross-flow filtrations. Both modes, cross-flow and dead-end, showed that a deposit on the membrane is formed as well as the same amount of fouling is detectable (in terms of resistance in cross-flow mode, and in terms of $\log(d^2t/dV^2)$ for dead-end mode). In fact, as explained before, the $\log(d^2t/dV^2)$ ($\frac{d^2t}{dV^2} = \frac{d}{dV}\left(\frac{1}{Q}\right)$ with $Q = \frac{\Delta PS}{\mu R}$) represents the variation of the hydraulic resistance with the filtered volume. When comparing the $\log(d^2t/dV^2)$ and the total hydraulic resistance for both tested transmembrane pressure, the two filtrations present the same evolution and almost the same amount of total resistance as well as the same evolution and amount of $\log(d^2t/dV^2)$.

In the case of FW added with 2.5 g/l tannins, the value of the blocking index (n) varies over time. At 0.5 bar, the first recorded value of the blocking index (n = 0.5) means that there is a transition between two models: intermediate pore blocking and cake filtration. The transition leads to cake filtration model (n = 0). At 1×10^5 Pa, the beginning of the filtration shows a blocking index equal to 1 characteristic of the intermediate pore blocking. This latter is followed by a transition (n = 0.5) to the cake filtration model (n = 0). The end of the filtration is characterized by a negative blocking index. In our case and as Iritani, Mukai, Tanaka, and Murase (1995) have shown in their study, the negative slope contradicts the theory.

It should be noted that the membrane has a non-homogeneous pore size distribution. Thus, fouling does not occur in the same way and at the same rate on every pore. These distributions may partly explain why there is no clear separation between fouling models.

It was surprising to find that tannins could form a deposit during microfiltration because these molecules ($DP_m \approx 5.5$) have a size range below the membrane cut-off (0.2 μm). Tannins are unstable molecules and their physical–chemistry aspect behavior is not well known yet. Several authors have shown that tannins can self-associate and eventually aggregate to form colloidal particles (Poncet-Legrand et al., 2003; Riou, Vernhet, Doco, and Moutounet, 2002). So, the cake formation by tannin molecules could be induced by the convective flux. This latter can enhance the physical–chemical interactions between tannin molecules leading to aggregation phenomena. According to our observations, the most plausible mechanism is a fast interaction between tannins and the membrane (adsorption), quickly followed by tannin–tannin interactions leading to aggregates that could block the pores and then form a deposit at the membrane surface.

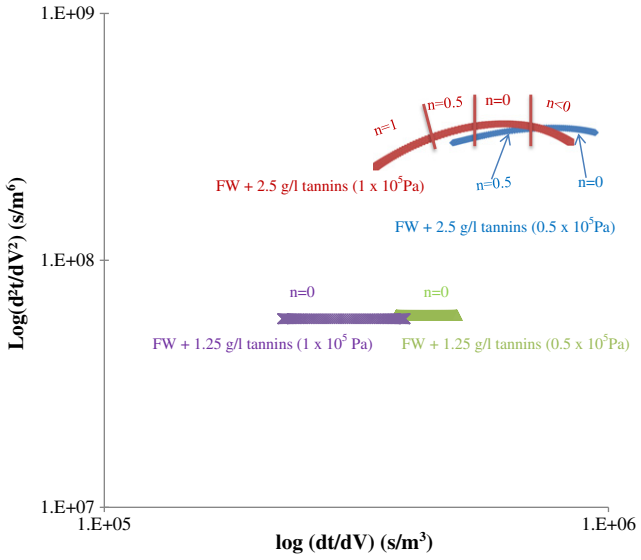

Fig. 7. A plot of d^2t/dV^2 vs. dt/dV curves for wine added with tannins.

4.2. Effect of added polysaccharides

The impact of wine polysaccharides on filtration performances was studied by testing two categories of polysaccharides. The first category includes pectin which comes from grape berries. The second category is formed by mannoproteins whose presence in wine is due to the release from yeast cell wall.

4.2.1. Pectins impact on cross-flow filtration performances

Fig. 8 shows the experimental data of the permeate fluxes as a function of filtered volume during constant ΔP (0.5 and 1×10^5 Pa) cross-flow microfiltration for wines containing pectins at different concentrations (0.25 and 0.5 g/l). Transmembrane pressure seems to only affect the initial permeate flux. At the end of the filtrations, no real differences have been noticed in terms of permeate flux for wines containing 0.25 and 0.5 g/l pectins when increasing the transmembrane pressure. Results showed a severe fouling comparing to filtrations with FW alone. The presence of pectins had a noticeable influence even from the first seconds of filtration independently of pectin concentration. This assumption was confirmed by a last trial with the pectin concentration divided by 5 (0.05 g/l) compared to the initial lowest tested concentration (0.25 g/l). At 0.5 bar, mean permeate flux observed for wines containing pectins ranges between 75% (FW + 0.05 g/l pectin) and 85% (FW + 0.5 g/l pectin) lower than the mean permeate flux of the FW.

The total resistance (Fig. 9) of all wines added with pectins increases during filtration. As for wines containing tannins, a gradual decrease in slope is observed which means that an external fouling is taking place. The total resistance behavior for all filtrations doesn't contain any point of inflection or concavity upwards. So, the mechanism proposed to explain membrane fouling appears to be an immediate fouling of the pores and a growing pectin layer onto membrane surface. This mechanism seems to be in accordance with several other works dealing with pectins but not specific to wine (Jiraratananon, Uttapap, and Tangamornusksun, 1997; Rai, Majumdar, Dasgupta, and De, 2005; Riedl, Girard, and Lencki, 1998). The experimental data clearly show that the total resistance increases with an increase in pectin concentration and transmembrane pressure. Total resistance is quickly stabilized and reached the quasi-steady state for a filtered volume of 0.0015 m^3, regardless of the operating conditions and the type of filtered solution. At 1×10^5 Pa, wine containing 0.5 g/l pectins reached a total resistance 10 times higher than that

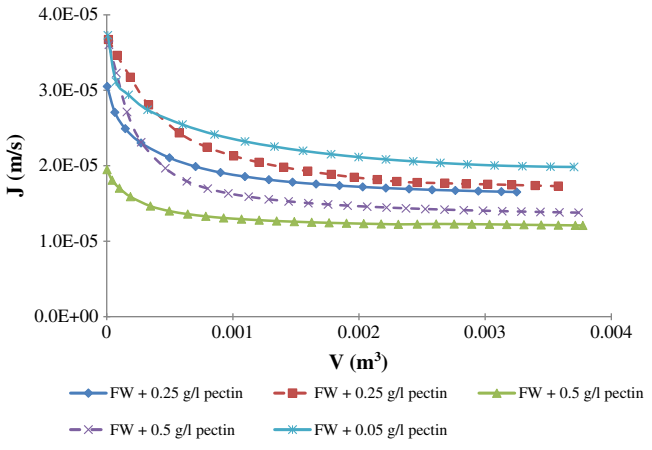

Fig. 8. Permeate flux versus permeate volume data obtained during cross-flow microfiltration of wines added with pectins (—: 0.5×10^5 Pa; ---: 1×10^5 Pa).

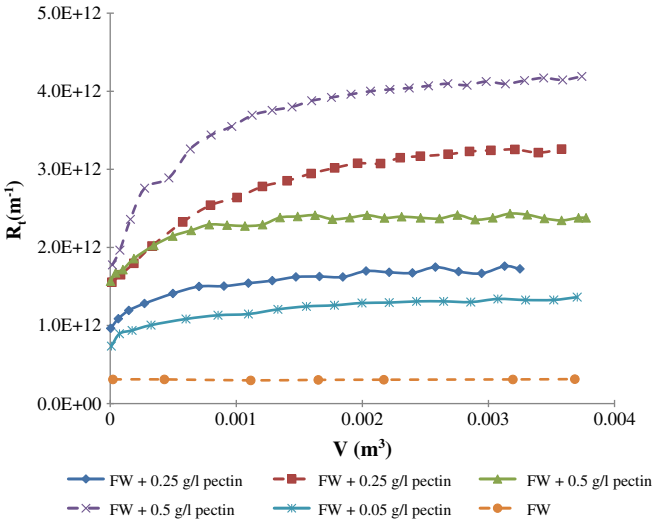

Fig. 9. Total hydraulic resistance during wine filtrations containing pectins at different concentrations (0.05, 0.25 and 0.5 g/l) and transmembrane pressures (0.5 and 1×10^5 Pa) (—: 0.5×10^5 Pa; ---: 1×10^5 Pa).

obtained with FW at the same pressure. The effect of transmembrane pressure is clearer when plotting the total resistance more than the representation of permeate flux. For wines containing 0.25 and 0.5 g/l pectins, an increase in ΔP from 0.5 to 1×10^5 Pa doubled approximately the total resistance. At high ΔP, the rate of deposition of pectins would be high leading to a thick deposit and gelification. The high pressure may also compress the deposit into a denser fouling layer as shown also by El Rayess, Albasi, Bacchin, Taillandier, Mietton-Peuchot, et al. (2011a).

4.2.2. Mannoprotein impact on cross-flow filtration performances

Mannoproteins are polysaccharides originating from the yeast cell wall. Among wine polysaccharides, it was shown that mannoproteins play crucial roles in membrane fouling during wine filtration (Vernhet, Pellerin, Belleville, Planque, and Moutounet, 1999). In our following filtration experiments, the aim was to describe the behavior of FW + mannoprotein solutions on a ceramic membrane with a mean cut-off of 0.2 μm. For the first time, the behavior of mannoproteins was investigated using wines added with mannoproteins at concentrations of 0.1 and 0.2 g/l at 0.5 bar (range of concentrations found in wine). The results presented in Fig. 10 indicate a significant effect of mannoproteins on the permeate flux. However, the two tested concentrations exhibited approximately the same permeate flux. So, there were no differences between the two tested concentrations in terms of permeate flux and even in total resistance (Fig. 11). This observation led us to suggest that there is a mannoprotein effect independently of its concentration. In order to confirm this suggestion, a wine containing 0.02 g/l mannoproteins was filtered at the same pressure. This wine exhibited permeate fluxes two times higher than those obtained with 0.2 g/l mannoproteins. This result shadowed our previous suggestion and the filtrations of wines added with mannoproteins are well mannoprotein concentration dependant. It also seems that there is a limit concentration above which a plateau value of permeate flux is obtained. Further experiments are needed to determine accurately this limit concentration which seems to be lower than 100 mg/l in our case.

The transmembrane pressure effect (0.5 and 1×10^5 Pa) was only tested on wines containing 0.2 g/l mannoproteins. As it can be seen on Fig. 10, an increase in ΔP (1×10^5 Pa) enabled an increase in initial permeate flux. On the other hand, a rapid decrease in fluxes is observed and values at the end of the filtration are lower than those obtained at 0.5×10^5 Pa.

When plotting the total resistance versus filtered volume, wines containing 0.02 g/l mannoproteins exhibited lower total resistance for $\Delta P = 0.5\times10^5$ Pa while 0.1 and 0.2 g/l have similar total resistance evolution at the same pressure. When increasing ΔP to 0.5 and 1×10^5 Pa, the curve seems to have an inflection point around 0.0015 m^3. This latter means that there is a transition between a concave up curve involving a pore constriction mechanism and a concave down implying a cake layer formation (Tracey and Davis, 1994).

4.2.3. Fouling mechanisms

The fouling mechanisms during filtration of wines loaded with polysaccharides have been studied for the following solutions: FW + 0.2 g/l mannoproteins and FW + 0.25 g/l pectins at 0.5 and 1×10^5 Pa.

4.2.3.1. Mechanism identification by linearized forms. The obtained R^2 of the linearized forms for the different blocking models obtained during filtration of these solutions are shown in Table 3. The cake filtration model can be applied to the following filtrations: FW + 0.2 g/l mannoproteins (0.5×10^5 Pa), FW + 0.25 g/l pectins (0.5×10^5 Pa) and FW + 0.25 g/l pectins (1×10^5 Pa). The resistance coefficient (K_g) of FW + 0.25 g/l pectins increased by 10 times fold when doubling the transmembrane pressure. This means that the cake formed by pectins is a compressible deposit which may explain the lower permeate flux obtained with wines added by pectins.

On the other hand, the succession of three blocking models (complete pore blocking ($r^2 = 0.9954$), intermediate pore blocking ($r^2 = 0.9982$) and standard pore blocking ($r^2 = 0.9905$)) may

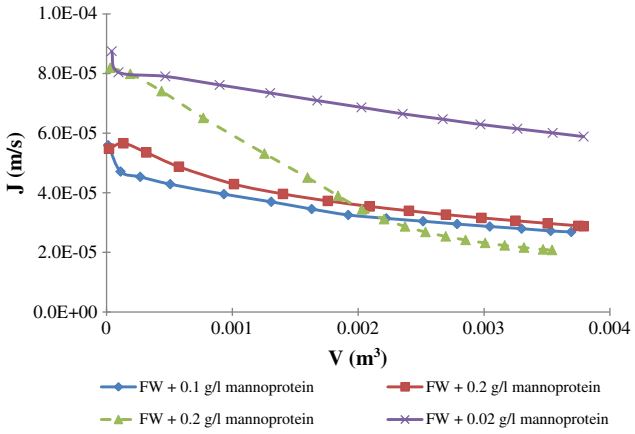

Fig. 10. Permeate fluxes versus permeate volume during wine filtration added with mannoproteins (—: 0.5×10^5 Pa; ---: 1×10^5 Pa).

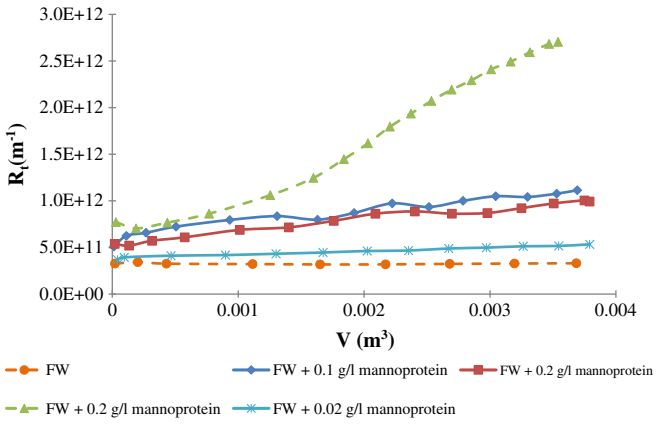

Fig. 11. Total resistance versus permeate volume during wine filtration added with mannoproteins (—: 0.5×10^5 Pa; ---: 1×10^5 Pa).

Table 3
Summary of parameters associated to various blocking models for FW added with polysaccharides.

	Complete pore blocking		Intermediate pore blocking		Standard pore blocking		Cake filtration	
	r^2	K_c (m^{-1})	r^2	K_i (m^{-1})	r^2	K_s ($m^{-1/2}/s^{-1/2}$)	r^2	K_g (s/m^2)
FW + 0.2 g/l mannoproteins (0.5×10^5 Pa)	0.969		0.948		0.965		0.995	1.44×10^6
FW + 0.2 g/l mannoproteins (1×10^5 Pa)	0.995	9.2×10^{-4}	0.998	20.41	0.99	6.7×10^{-2}	0.965	
FW + 0.25 g/l pectins(0.5×10^5 Pa)	0.969		0.946		0.917		0.995	2.15×10^6
FW + 0.25 g/l pectins(1×10^5 Pa)	0.969		0.939		0.898		0.998	2.26×10^7

illustrated the fouling mechanisms for the FW + 0.2 g/l mannoprotein (1 bar) solution.

4.2.3.2. Mechanism identification by d^2t/dV^2. In order to investigate the coexistence of fouling mechanisms, d^2t/dV^2 vs. dt/dV curves for FW added with polysaccharides are presented on Fig. 12. Results show that only the cake filtration model (n = 0) is representative of the fouling mechanisms during filtration of wines added with pectins. These results confirm those obtained with the linearized form. Cross-flow filtration of the same solutions reported also cake layer formation. In fact, the amount of fouling (in terms of total resistance in cross-flow mode, and in terms of $\log(d^2t/dV^2)$ in dead-end mode) is higher when filtering at pressure 1×10^5 Pa than 0.5×10^5 Pa. For both studied pressures, it is noticed that the amount of fouling is proportional to the applied pressure in cross-flow mode, while in dead-end, an amount of fouling 10-times higher is observed when increasing the pressure. This latter observation may be due to a compressible deposit formed by the pectins and to a bigger rate of deposition at 1×10^5 Pa.

In the literature, the cake filtration mechanism is well identified during the filtration of fruit juices loaded with pectins and polysaccharides (Nandi, Das, Uppaluri, and Purkait, 2011; Rai, Majumdar, Dasgupta, and De, 2006). It was described by the formation of a gel-type layer on the membrane surface adding a supplemental hydraulic resistance (Kirk, Montgomery, and Kortekaas, 1983; Vladisavljevic, Vukosavljevic, and Bukvic, 2003). The pectins used in this study (citrus pectins, Sigma, P9135) have an esterification degree of 60.9% therefore it belongs to the highly methylated pectins (Sato, Oliveira, and Cunha, 2008). This latter can form a gel in acidic medium (pH<3.8) through hydrogen bonds and hydrophobic interactions. The formation of this gel-type layer is enhanced by the process especially by increasing the transmembrane pressure and thus the convective flux (Rai et al., 2006).

Fig. 12 also illustrates the results obtained during filtration of wines added with 0.2 g/l mannoproteins. Results reveal that only the cake filtration mechanism (n = 0) is present at 0.5 bar while several mechanisms manifest at 1 bar. The first mechanism presents a blocking index higher than 2 (n = 3.8) which is not identified in the literature but would suggest that a small amount of molecules block some pores. Then, the complete blocking (n = 2) model is identified followed by the intermediate blocking model corresponding to molecules beginning to settle on other retained molecules. The end of the filtration seems to be governed by cake layer formation. These results are consistent with those obtained from the linearized forms. They can also explain the unusual shape of the total resistance curve obtained from the filtration of the same solution in cross-flow mode (Fig. 11). In cross-flow filtration of the same solution, an inflection point in the total resistance curve was observed and reported as a transition between several fouling mechanisms. These mechanisms have been identified by the analysis of fouling in dead-end mode: complete blocking and intermediate blocking mechanism and cake layer formation. A transition in blocking mechanisms was also observed by Ye, Le Clech, Chen, Fane, and Jefferson (2005) during filtration of model solution of extracellular polymeric substances (EPS). They showed that the beginning of the filtration was governed by the standard blocking mechanism followed by a cake layer formation.

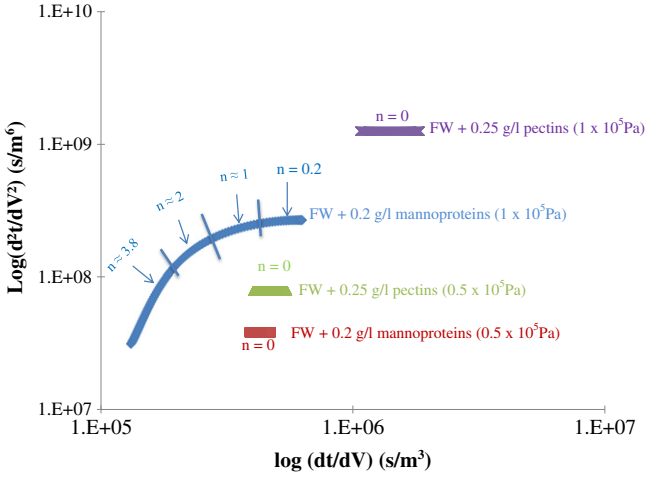

Fig. 12. d^2t/dV^2 vs. dt/dV curves for FW added with polysaccharides (0.2 g/l mannoproteins or 0.25 g/l pectins).

4.3. Analysis of the initial fluxes

In this section, the initial fluxes (Table 4) obtained during all conducted filtrations will be discussed. In fact, experiments performed with FW at 0.5×10^5 Pa should record an initial flux around 0.8×10^{-4} m/s and 1.8×10^{-4} m/s for those conducted at 1×10^5 Pa. This is not the case for all filtrations where the initial flux value is a function of the type of added molecules, the associated concentrations and the applied pressure. It must be mentioned that a maximum of 10% difference of membrane water permeability is tolerated after chemical cleaning. So, the membrane has almost the same permeability at the beginning of each filtration.

For wines added with tannins as well as those added with mannoproteins, initial fluxes (regardless of the applied pressure) seem to be concentration dependent. For example, the initial fluxes of FW + 1.25 g/l tannins fit well with expectations while those obtained with 2.5 g/l tannins are divided by half, sign of a very quick fouling. The initial fluxes recorded with 0.1 g/l and 0.2 g/l mannoproteins are below those obtained with FW. At 0.02 g/l mannoproteins, the initial flux (8.2×10^{-5} m/s) matches well with the expected one. These observations are in accordance with the flux evolution, for which an influence of the concentration, probably based on physical–chemical considerations has been pointed out.

The effect of pectins is noticeable from the very first seconds of filtration. Any of the 5 experiments conducted in the presence of pectins showed the expected initial fluxes whatever the used concentration. The initial flux was improved when adding enzymes but still did not reach the desired value of FW. The strong affinity of pectins with membrane is here confirmed.

In conclusion, although the initial fluxes are closely related to the state of the membrane, it is obvious and surprising that the nature of filtered molecules and their concentration had an immediate effect on these fluxes during wine filtration.

Table 4
Summary of the initial fluxes obtained with different filtrations (n.d. = not determined).

	FW	Initial flux (10^{-5} m/s)				
		FW + 1.25 g/l tannins	FW + 2.5 g/l tannins	FW + 0.1 g/l mannoproteins	FW + 0.2 g/l mannoproteins	FW + 0.02 g/l mannoproteins
0.5×10^5 Pa	8	7.62	3.22	5.59	5.48	8.2
1×10^5 Pa	18	18	6.65	n.d.	8.19	n.d.

	Initial flux (10^{-5} m/s)		
	FW + 0.25 g/l pectins	FW + 0.5 g/l pectins	FW + 0.05 g/l pectins
0.5×10^5 Pa	3.73	1.95	3.7
1×10^5 Pa	3.67	3.6	n.d.

4.4. Influence of cross-flow microfiltration on chemical composition of wines

Analytical measurements carried out on samples from feed and permeate of the cross-flow microfiltration of wines are reported in Table 5. The wine characteristics as pH, % of ethanol, total acidity and total anthocyanin were affected neither by the added compounds nor by the process. These parameters were 3.6, 12.07%, 2.48 g/l H_2SO_4 and 350–360 mg/l, respectively. The value of total acidity is low because the wines undergo malolactic fermentation and tartaric acid stabilization.

Regardless of the initial turbidity of the wine, the permeate turbidity is always inferior to 1.5 NTU. This means that cross-flow microfiltration fulfilled its mission and had lowered wine turbidity less than 2 NTU.

When adding tannins to the wines, an increase in turbidity, color intensity (IC), total polyphenol index (TPI) and total tannins is observed depending on the added concentration. For wines containing 1.25 or 2.5 g/l tannins, a decrease of 3.2–5% or 7.5% in IC, 3.4–6.2% or 5.6–6.2% in TPI and 7.4–8.6% or 5.6–7.6% in total tannins is observed after filtration. So, no significant differences in terms of quality loss are observed between both tested concentrations.

According to Arriagada-Carrazana, Saez-Navarrete, and Brodeu (2005), the reduction observed in TPI, IC and the decrease in the concentration of tannins can be explained by the adsorptive phenomenon of tannins on membrane material. The adsorptive phenomenon was also highlighted by Vernhet and Moutounet (2002) and Ulbricht et al. (2009). However, interactions between macromolecules induced by hydrodynamic conditions must be taken into consideration. These interactions lead to macromolecular aggregation at pore entrance or membrane surface.

Concerning wines containing pectins, no changes were observed to IC, TPI and total tannins. Logically, an increase in total polysaccharides has been observed depending on the added concentration. Permeates were impoverished in polysaccharide concentration due to the retention of pectins by the membrane and formation of a gel layer. This decrease is about 33–35% for wines supplemented with 0.25 g/l pectins and 34–42% for those added with 0.5 g/l pectins. Enzyme treated wines showed lower initial concentration (about 20–22%) in total polysaccharides. Concentration of total polysaccharides in permeates of wines treated with enzyme decreased by about 32%. This latter percentage is the same for permeates of wines supplemented with 0.2 g/l mannoproteins.

Supplemented wines with mannoproteins as wines containing pectins showed no changes to IC, TPI and total tannins. A decrease in total polysaccharides is observed after filtration. It is about 16% for wines containing 0.1 g/l mannoproteins and 32–33% for wines containing 0.2 g/l mannoproteins.

5. Conclusion

In this study, the tested wine constituents: tannins, pectins and mannoproteins induced permeate flux declines but with different impacts on membrane fouling. Filtered wine (FW) induced a little loss of membrane permeability, due to the adsorption of wine molecules on membrane material. Wine colloids had a strong impact on membrane fouling. Independently of their concentrations found in wine, they can be ranked according to their increasing effect on permeate flux as: mannoproteins < tannins < pectins.

Quick adsorption followed by pore blocking and/or aggregation and ending by a cake formation is the most plausible mechanism to explain fouling by wine tannins. The strong impact of pectins is due to the formation of the gel layer at the membrane surface. The coexistence of different fouling mechanisms was highlighted with wines containing mannoproteins but the ends of the filtrations are governed by the cake layer filtration mechanisms.

Table 5
Analytical composition of different wines before and after filtration.

				Turbidity (NTU) (±0.2)			IC (±0.07)		IPT (±0.5)		Tannins (g/l) (±0.12)			Polysaccharides (mg/l) (±30)		
				Feed	Permeate	% removal	Feed	Permeate	Feed	Permeate	Feed	Permeate	% removal	Feed	Permeate	% removal
FW	Tannins	1.25 g/l	0.5×105 Pa	0.1	0.1	0	0.85	0.84	44.5	44.2	2.45	2.43	0.8	60	54	10
				38.7	0.9	98	0.93	0.9	58.5	56.5	3.48	3.22	7.5	70	55	21
			0.5×10^5 Pa	39.2	1.1	97	0.94	0.89	59.3	55.6	3.45	3.15	8.7	50	60	0
		1.25 g/l	0.5×105 Pa	73.2	1.2	98	1.01	0.93	72.1	67.7	4.55	4.28	6	72	63	12.5
			1×105 Pa	71.3	1.5	98	1.02	0.94	72.4	68.3	4.6	4.25	7.5	80	59	26
		0.25 g/l	0.5×105 Pa	12.2	0.7	94	0.86	0.84	44.5	43.7	2.45	2.4	2	315	205	35
			0.5×10^5 Pa	12.8	0.6	95	0.87	0.85	46.3	44.2	2.48	2.42	2.5	305	205	33
	Pectins	0.5 g/l	0.5×105 Pa	22.3	0.5	98	0.87	0.85	46.8	43.8	2.52	2.4	5	535	350	34.5
			1×105 Pa	21.4	1.1	95	0.87	0.84	46.5	43.9	2.53	2.41	4.7	550	320	42
		0.25 g/l + enz.	1×105 Pa	19.6	1.02	95	0.86	0.84	46.2	45.2	2.6	2.45	5.7	210	150	28.5
	Mannoproteins	0.1 g/l	0.5×105 Pa	3.2	0.28	97	0.85	0.85	45.8	45.2	2.38	2.36	0.8	190	160	16
		0.2 g/l	0.5×105 Pa	6.22	0.68	89	0.85	0.84	44.7	44.8	2.4	2.39	0.4	315	215	32
			1×105 Pa	6.8	1.2	82	0.86	0.84	45.3	44.9	2.38	2.35	1.3	285	190	33

The analytical measurement showed that cross-flow microfiltration may induce a loss till 8% in total tannins, 6% in TPI and 35% in total polysaccharides. The loss in total polysaccharides may affect the quality of wine but more studies with real wines are needed to assess this point.

No relationship was found between the initial turbidity and filtration performances. So, new parameter or index is necessary to predict filtration performances of wines.

Nomenclature

d^2t/dV^2	variation of the hydraulic resistance with the filtered volume
n	blocking index
K_c	resistance coefficient of complete pore blocking model (m^{-1})
K_s	resistance coefficient of standard pore blocking model ($m^{-1/2}/s^{-1/2}$)
K_i	resistance coefficient of intermediate pore blocking model (m^{-1})
K_g	resistance coefficient of cake filtration model (s/m^2)
K_A	blocked surface of the membrane per unit of filtered volume that flow through the membrane (m^{-1})
K_B	cross section blocked surface per unit of total volume that flow through the membrane (m^{-1})
K_D	cake surface per unit of total volume which flow through the membrane (m^{-1})
R_g	hydraulic resistance due to the cake formation (m^{-1})
R_m	membrane hydraulic resistance (m^{-1})
A	membrane surface blocked at time t (m^2)
A_0	initial membrane surface (m^2)
J_0	the initial permeate flux (m/s)
J	permeate flux (m/s)
V	filtered volume (m^3)
t	time (s)
S	membrane surface (m^2)
ΔP	transmembrane pressure (Pa)
μ	wine viscosity (Pa.s)
R_t	total hydraulic resistance (m^{-1})

Acknowledgments

The authors gratefully acknowledge “PERA” company and Centre National de Recherche Scientifique (CNRS) for their financial support.

References

Arriagada-Carrazana, J. P., Saez-Navarrete, C., & Brodeu, E. (2005). Membrane filtration effects on aromatic and phenolic quality of Cabernet Sauvignon wines. *Journal of Food Engineering*, *68*(3), 363–368.

Belleville, M. P., Brillouet, J. M., Tarodo de la Fuente, B., & Moutounet, M. (1992). Fouling colloids during microporous alumina membrane filtration of wine. *Journal of Food Science*, *57*(2), 396–400.

Boissier, B., Lutin, F., Moutounet, M., & Vernhet, A. (2008). Particles deposition during the cross-flow microfiltration of red wines—Incidence of the hydrodynamic conditions and of the yeast to fines ratio. *Chemical Engineering and Processing: Process Intensification*, *47*(3), 276–286.

Bowen, W. R., Calvo, J. I., & Hernandez, A. (1995). Steps of membrane blocking in flux decline during protein microfiltration. *Journal of Membrane Science*, *101*(1–2), 153–165.

Czekaj, P., Lopez, F., & Guell, C. (2000). Membrane fouling during microfiltration of fermented beverages. *Journal of Membrane Science*, *166*(2), 199–212.

El Rayess, Y., Albasi, C., Bacchin, P., Taillandier, P., Mietton-Peuchot, M., & Devatine, A. (2011). Cross-flow microfiltration of wine: Effect of colloids on critical fouling conditions. *Journal of Membrane Science*, *385–386*(1), 177–186.

El Rayess, Y., Albasi, C., Bacchin, P., Taillandier, P., Raynal, J., Mietton-Peuchot, M., & Devatine, A. (2011). Cross-flow microfiltration applied to oenology: A review. *Journal of Membrane Science*, *382*(1–2), 1–19.

Flanzy, C. (1998). *Œnologie: Fondements scientifiques et technologiques.* Paris: Lavoisier TEC&DOC.

Grenier, A., Meireles, M., Aimar, P., & Carvin, P. (2008). Analysing flux decline in dead-end filtration. *Chemical Engineering Research and Design*, *8*(11), 1281–1293.

Hermans, P. H., & Bredee, H. L. (1936). Principles of the mathematical treatment of constant pressure filtration. (Pappas). *Journal of Society of Chemical Industry*, *55*(1), 1–11.

Hermia, J. (1982). Constant pressure blocking filtration laws—Application to power-law non-Newtonian fluids. *Transaction of the Institution of Chemical Engineers*, *60*, 183–187.

Iritani, E., Mukai, Y., Tanaka, Y., & Murase, T. (1995). Flux decline behavior in dead-end microfiltration of protein solutions. *Journal of Membrane Science*, *103*(1–2), 181–191.

Jiraratananon, R., Uttapap, D., & Tangamornusksun, C. (1997). Self-forming dynamic membrane for ultrafiltration of pineapple juice. *Journal of Membrane Science*, *129*(1), 135–143.

Kirk, D. E., Montgomery, M. W., & Kortekaas, M. G. (1983). Clarification of pear juice by hollow fiber ultrafiltration. *Journal of Food Science*, *48*(6), 1663–1667.

Nandi, B. K., Das, B., Uppaluri, R., & Purkait, M. K. (2009). Microfiltration of mosambi juice using low cost ceramic membrane. *Journal of Food Engineering*, *95*(4), 597–605.

Nandi, B. K., Das, B., Uppaluri, R., & Purkait, M. K. (2011). Identification of optimal membrane morphological parameters during microfiltration of mosambi juice using low cost ceramic membranes. *LWT— Food Science and Technology*, *44*(1), 214–223.

Poirier, D., Bennasar, M., Tarodo de la Fuente, B., Gillot, J., & Garcera, D. (1984). Clarification et stabilisations des vins par ultrafiltration tangentielle sur membranes minérales. *Le Lait*, *64*(638–639), 141–142.

Poncet-Legrand, C., Cartalade, D., Putaux, J. L., Cheynier, V., & Vernhet, A. (2003). Flavan-3-ol aggregation in model ethanolic solutions: Incidence of polyphenol structure, concentration, ethanol content and ionic strength. *Langmuir*, *19*(25), 10563–10572.

Preys, S., Souquet, J. M., Meudec, E., Morel-Salmi, C., & Cheynier, V. (2004). Development of a rapid quantative method to analyse proanthocyanidins in red wines. (25–28 August 2004, Helsinki, Finland). *Proceedings of XXII International Conference on Polyphenols* (pp. 25–28).

Rai, P., Majumdar, G. C., Dasgupta, S., & De, S. (2005). Understanding ultrafiltration performance with mosambi juice in an unstirred batch cell. *Journal of Food Process Engineering*, *28*(4), 166–180.

Rai, P., Majumdar, G. C., Dasgupta, S., & De, S. (2006). Modeling of sucrose permeation through a pectins gel during ultrafiltration of depectinsized mosambi [*Citrus sinensis* (L.) Osbeck] juice. *Journal of Food Science*, *71*(2), 87–94.

René, F., & Lalande, M. (1991). Momentum and mass transfer during ultrafiltration of dextran with tubular mineral membranes in turbulent flow regime. *Journal of Membrane Science*, *56*(1), 29–48.

Ribéreau-Gayon, P., Glories, Y., Maujean, A., & Dubourdieu, D. (2006). *Handbook of enology* (2nd ed.). *The chemistry of wine, stabilization and treatments.*, *2*, Paris: Dunod.

Riedl, K., Girard, B., & Lencki, R. W. (1998). Influence of membrane structure on fouling layer morphology during apple juice clarification. *Journal of Membrane Science*, *139*(2), 155–166.

Riou, V., Vernhet, A., Doco, T., & Moutounet, M. (2002). Aggregation of grape seed tannins in model wine — Effect of wine polysaccharides. *Food Hydrocolloids*, *16*(1), 17–23.

Salazar, F. N., de Bruijn, J. P. F., Seminario, L., Guell, C., & Lopez, F. (2007). Improvement of wine crossflow microfiltration by a new hybrid process. *Journal of Food Engineering*, *79*(4), 1329–1336.

Sato, A. C. K., Oliveira, P. R., & Cunha, R. L. (2008). Rheology of mixed pectins solutions. *Food Biophysics*, *3*(1), 100–109.

Tracey, E. M., & Davis, R. H. (1994). Protein fouling of track-etched polycarbonate microfiltration membranes. *Journal of Colloid and Interface Science*, *167*(1), 104–116.

Ulbricht, M., Ansorge, W., Danielzik, I., Konig, M., & Schuster, O. (2009). Fouling in microfiltration of wine: The influence of the membrane polymer on adsorption of polyphenols and polysaccharides. *Separation and Purification Technology*, *68*(3), 335–342.

Usseglio-Tomasset, L. (1976). Les colloïdes glucidiques solubles des moûts et des vins. *Connaissance de la vigne et du vin*, *10*(2), 193–226.

Vernhet, A., Cartalade, D., & Moutounet, M. (2003). Contribution to the understanding of fouling build-up during microfiltration of wines. *Journal of Membrane Science*, *211*(2), 357–370.

Vernhet, A., & Moutounet, M. (2002). Fouling of organic microfiltration membranes by wine constituents: Importance, relative impact of wine polysaccharides and polyphenols and incidence of membrane properties. *Journal of Membrane Science*, *201*(1–2), 103–122.

Vernhet, A., Pellerin, P., Belleville, M. P., Planque, J., & Moutounet, M. (1999). Relative impact of major wine polysaccharides on the performances of an organic microfiltration membrane. *American Journal of Enology and Viticulture*, *50*(1), 51–56.

Vladisavljevic, G. T., Vukosavljevic, P., & Bukvic, B. (2003). Permeate flux and fouling resistance in ultrafiltration of depectinsized apple juice using ceramic membranes. *Journal of Food Engineering*, *60*(3), 241–247.

Ye, Y., Le Clech, P., Chen, V., Fane, A. G., & Jefferson, B. (2005). Fouling mechanisms of alginate solutions as model extracellular polymeric substances. *Desalination*, *175*(1), 7–20.